

Dispersion compensation in an Yb-doped fiber oscillator for generating transform-limited, wing-free pulses

Takashi Kurita,^{1,2,3,*} Hidetsugu Yoshida,¹ Hiroaki Furuse,⁴ Toshiyuki Kawashima,^{2,3}
and Noriaki Miyanaga^{1,3}

¹*Institute of Laser Engineering, Osaka University, 2-6 Yamada-oka, Suita, Osaka 565-0871, Japan*

²*Hamamatsu Photonics K. K., 1820 Kurematsu-cho, Nishi-ku Hamamatsu, Shizuoka 431-1202, Japan*

³*Japan Science and Technology Agency, CREST, 2-6 Yamada-oka, Suita, Osaka 565-0871, Japan*

⁴*Institute for Laser Technology, 2-6 Yamada-oka, Suita, Osaka 565-0871, Japan*

*t-kurita@crl.hpk.co.jp

Abstract: We investigate the effect of dispersion compensation on temporal characteristics in mode-locking by nonlinear polarization rotation in an ytterbium-doped fiber (YDF) oscillator with intracavity and external grating pairs. A short fixed length YDF was spliced with a longer single-mode fiber (SMF). Using experimentally measured dispersion characteristics of the YDF, SMF and cavity optics, we control the group velocity dispersion (GVD) and spectral broadening in a cavity by changing the SMF length. As a result, the oscillator generated 29.4-fs transform-limited wing-free pulses, which are to our knowledge the shortest and cleanest pulses achieved without the use of additional optics like a prism pair for high-order dispersion compensation. The results show that a precise balance of higher order terms of the GVD and self-phase modulation is essential for shortening pulse duration.

©2011 Optical Society of America

OCIS codes: (140.3510) Lasers, fiber; (320.7090) Ultrafast lasers.

References and links

1. W. H. Loh, D. Atkinson, P. R. Morkel, M. Hopkinson, A. Rivers, A. J. Seeds, and D. N. Payne, "All-solid-state subpicosecond passively mode locked erbium-doped fiber laser," *Appl. Phys. Lett.* **63**(1), 4–6 (1993).
2. K. Tamura, E. P. Ippen, H. A. Haus, and L. E. Nelson, "77-fs pulse generation from a stretched-pulse mode-locked all-fiber ring laser," *Opt. Lett.* **18**(13), 1080–1082 (1993).
3. A. Hideur, T. Chartier, M. Brunel, S. Louis, C. Özkul, and F. Sanchez, "Generation of high energy femtosecond pulses from a side-pumped Yb-doped double-clad fiber laser," *Appl. Phys. Lett.* **79**(21), 3389–3391 (2001).
4. B. Ortaç, J. Limpert, and A. Tünnermann, "High-energy femtosecond Yb-doped fiber laser operating in the anomalous dispersion regime," *Opt. Lett.* **32**(15), 2149–2151 (2007).
5. F. Ilday, J. Buckley, L. Kuznetsova, and F. Wise, "Generation of 36-femtosecond pulses from a ytterbium fiber laser," *Opt. Express* **11**(26), 3550–3554 (2003).
6. J. R. Buckley, S. W. Clark, and F. W. Wise, "Generation of ten-cycle pulses from an ytterbium fiber laser with cubic phase compensation," *Opt. Lett.* **31**(9), 1340–1342 (2006).
7. X. Zhou, D. Yoshitomi, Y. Kobayashi, and K. Torizuka, "Generation of 28-fs pulses from a mode-locked ytterbium fiber oscillator," *Opt. Express* **16**(10), 7055–7059 (2008).
8. A. Komarov, H. Leblond, and F. Sanchez, "Multistability and hysteresis phenomena in passively mode-locked fiber lasers," *Phys. Rev. A* **71**(5), 053809 (2005).
9. K. Kieu, W. H. Renninger, A. Chong, and F. W. Wise, "Sub-100 fs pulses at watt-level powers from a dissipative-soliton fiber laser," *Opt. Lett.* **34**(5), 593–595 (2009).
10. S. M. Kelly, "Characteristics sideband instability of periodically amplified average soliton," *Electron. Lett.* **28**(8), 806–807 (1992).
11. A. Chong, W. H. Renninger, and F. W. Wise, "Properties of normal-dispersion femtosecond fiber lasers," *J. Opt. Soc. Am. B* **25**(2), 140–148 (2008).
12. R. H. Stolen and C. Lin, "Self-phase-modulation in silica optical fibers," *Phys. Rev. A* **17**(4), 1448–1453 (1978).
13. I. Amat-Roldán, I. G. Cormack, P. Loza-Alvarez, E. J. Gualda, and D. Artigas, "Ultrashort pulse characterisation with SHG collinear-FROG," *Opt. Express* **12**(6), 1169–1178 (2004).

14. D. J. Kane, G. Rodriguez, A. J. Taylor, and T. S. Clement, "Simultaneous measurement of two ultrashort laser pulses from a single spectrogram in a single shot," *J. Opt. Soc. Am. B* **14**(4), 935–943 (1997).
15. S. Zhou, L. Kuznetsova, A. Chong, and F. W. Wise, "Compensation of nonlinear phase shifts with third-order dispersion in short-pulse fiber amplifiers," *Opt. Express* **13**(13), 4869–4877 (2005).
16. D. N. Papadopoulos, Y. Zaouter, M. Hanna, F. Druon, E. Mottay, E. Cormier, and P. Georges, "Generation of 63 fs 4.1 MW peak power pulses from a parabolic fiber amplifier operated beyond the gain bandwidth limit," *Opt. Lett.* **32**(17), 2520–2522 (2007).

1. Introduction

In recent years there has been an increased demand for ultrashort-pulse laser systems for high-field science and technology. Mode-locked fiber lasers generating picosecond or femtosecond pulses have attracted considerable attention due to good beam quality and stability [1–4]. In particular, an ytterbium (Yb)-doped mode-locked fiber laser operating in the near-infrared is a suitable light source in such ultrashort pulse laser systems, because the spectrum matches the emission band of neodymium (Nd) and Yb-doped bulk materials for laser amplifiers. Several attempts have been made to minimize the pulse duration and to obtain a good temporal profile with Yb-doped fiber (YDF) oscillators. Ilday *et al.* optimized group velocity dispersion (GVD) values to obtain pulses as short as 36 fs without high-order dispersion compensation [5]. However, a considerable amount (~30%) of energy resided in the side lobe due to third-order dispersion ($\text{TOD} = \partial^3 \phi(\omega) / \partial \omega^3$, where $\phi(\omega)$ is the frequency-dependent phase of pulse). Buckley *et al.* demonstrated pulses as short as 33 fs with a clean temporal profile by use of a prism-grating sequence for third-order dispersion compensation [6]. Although Zhou *et al.* achieved a pulse duration of 28 fs for high-order dispersion compensation using a pair of prisms external to the cavity [7], small structures in the wings still remained.

To achieve shorter pulses with a good temporal profile, high-order dispersion control in the cavity is required, which leads to the complexity in laser systems and affects the output stability associated with alignment issues. In the laser setup in [5,6], a relatively long fiber length (4.2 m ~7.0 m) was used. On the other hand, the setup in [7] used a shorter fiber length (1.7 m), resulting in the shortest pulse duration. In general, it may be preferable for laser systems to consist of dispersive materials as short as possible. Therefore, the effects of the self-phase modulation and dispersion of the fibers on the pulse characteristics should be investigated to achieve shorter pulses with high quality. In this paper, we study the effects of the length of a single-mode fiber (SMF), which is used in combination with a YDF of fixed length, on the pulse characteristics. For this purpose, we experimentally measured the dispersion characteristics of the YDF, the SMF and the other optics to control the GVD in the cavity. Based on the GVD data, we optimized the fiber length to improve the temporal profile and minimize the pulse duration simultaneously. As a result, we generated pulses as short as 29.4 fs with a clean temporal profile using only two pairs of diffraction gratings for dispersion compensation.

2. Experimental setup and results

A schematic of the experimental setup is shown in Fig. 1. The oscillator included a 15-cm long YDF, a first SMF (SMF1) of variable length, a 27-cm long SMF (SMF2) and a 19-cm long SMF (SMF3). The core and clad diameters of the YDF were 3.8 μm (NA = 0.19) and 125 μm , respectively, and the absorption of the pump light was 2450 dB/m at 974 nm. The mode-field diameter and clad diameter of the SMFs were 6.2 μm (NA = 0.14) at 1060 nm and 125 μm , respectively. The losses of the fusion-spliced connections between the SMFs were less than 0.1 dB, and that of the connection between SMF2 and YDF was reduced to be less than 0.1 dB by optimizing the splicing conditions of arc power and time. The YDF was pumped by a fiber-coupled laser diode emitting at a wavelength of 976 nm with a maximum pump power of 300 mW. A 980/1060-nm wavelength division multiplexer (WDM) delivered the pump light to the YDF and ensured the propagation of the oscillating light in a wavelength range from 990 nm to 1120 nm. Considering the 0.6-dB insertion loss of the WDM, the

estimated pump power reaching the YDF was 260 mW. Two quarter-wave plates (QWP1 and QWP2), a half-wave plate (HWP) and a polarizer inside an optical isolator served as an artificial saturable absorber, realizing a passive mode-locked operation with nonlinear polarization rotation [8]. The optical isolator eliminated backward waves, which ensured unidirectional propagation. The GVD in the cavity was controlled by changing the length of SMF1, and by using a pair of reflection-type diffraction gratings (GP1) with a groove density of 600 lines/mm. A mode-locked pulse train was extracted by a polarizing beam splitter cube (PBS). The output pulse was positively chirped and dechirped externally by a pair of transmission gratings (GP2) with a thickness of 2 mm and a groove density of 600 lines/mm.

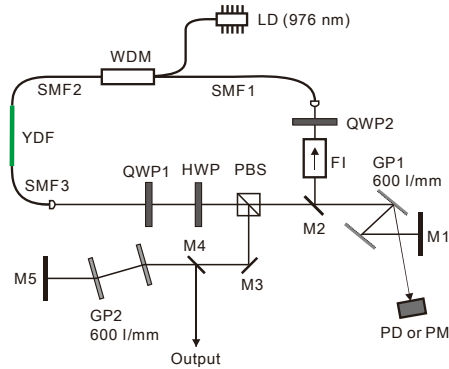


Fig. 1. Schematic of the YDF mode-locked oscillator. LD: laser diode; WDM: 980/1060-nm wavelength division multiplexer; SMF1-3: single-mode fibers; YDF: ytterbium-doped fiber; QWP1-2: quarter-wave plates; HWP: half-wave plate; PBS: polarizing beam splitter cube; FI: Faraday isolator; GP1: reflection grating pair; GP2: transmission grating pair; M: mirrors; PD: photodiode; PM: power meter.

As the distance between the gratings of GP1 was adjusted, the power spectrum changed according to the net GVD values in the cavity. The power spectrum with positive net GVD values showed steep spectral edges, indicating dissipative solitons [9]. For negative net GVD values, on the other hand, a characteristic spectrum with Kelly sidebands was observed [10]. As the net GVD approaches zero, shorter pulses are obtained as mentioned in [11]. Mode-locked operation can be obtained by adjusting the rotation angles of the HWP and QWP2, while that of QWP1 was kept constant. After mode-locked operation was realized, we adjusted the HWP to reduce the output power (to increase the intracavity power), resulting in spectral broadening due to enhanced self-phase modulation (SPM) [12]. The angle of QWP2 was then adjusted to obtain broader-band mode-locking. To monitor the pulse intensity, we measured the pulse train with a photodiode as shown in Figs. 2(b) and 2(c) by observing the specular reflection (zero-order diffraction illustrated in Fig. 1) from one of the gratings of GP1 in the cavity. The angular difference between the direction of the optical axis of the HWP and that of QWP2 was 3.0 degrees in the case without SPM, on the other hand, it was optimized to be 5.0 degrees in the case of the broadest bandwidth. Because the spectral broadening occurs mostly in optical fibers in the cavity, we can control it by changing the length of one of the optical fibers (SMF1).

A power meter was used to measure the average power of the specular reflection from GP1 to infer the intracavity power. The intracavity powers defined at the inlet of GP1 with and without SPM were estimated to be 33.1 mW (pulse energy of 334 pJ) and 18.3 mW (185 pJ), respectively. We measured the temporal width of the pulses extracted by the PBS using a second harmonic generation-based collinear FROG (SHG-CFROG) technique [13] and a principal component generalized projections (PCGP) phase-retrieval algorithm [14]. The pulse durations with and without SPM were 780 fs and 990 fs, respectively. As a result, the peak powers at the inlet of GP1 with and without SPM were estimated to be 0.43 kW and 0.19 kW, respectively. As expected from the principles of mode-locking for this oscillator, spectral

broadening occurred with increasing pulse amplitude. This indicates that the spectral phase is modified by SPM. We measured the corresponding temporal characteristics with and without spectral broadening using SHG-CFROG, as shown in Figs. 3(a) and 3(b), respectively. Transform-limited pulse shapes calculated from the power spectra shown in Fig. 2(a) are also shown. The pulse duration defined by the full-width at half-maximum (FWHM) was 29.4 fs, which is almost identical to that of the transform-limited pulse (29.2 fs). An output power of 57.9 mW (0.58-nJ pulse energy) at a repetition rate of 99 MHz was produced by 300-mW pump power. The dechirped pulse energy was 0.40 nJ, which corresponded to a conversion efficiency of 13% relative to the pump power. On the other hand, without the spectral broadening, we obtained a pulse duration of 50.1 fs (transform-limited pulse of 47.6 fs) with an output power of 72.5 mW (0.73-nJ pulse energy). It is important to note that the pedestal structures were substantially suppressed without using any optics with negative TOD. This is most likely because the nonlinear phase shift (NPS) due to SPM in fibers is attributed to the compensation of TOD [15].

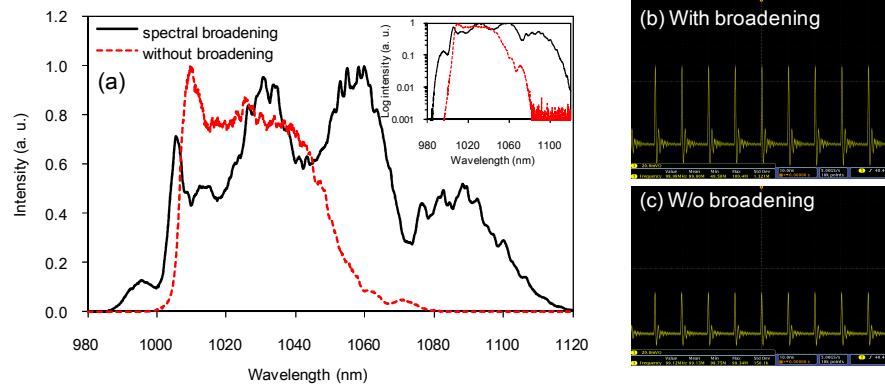


Fig. 2. (a) Power spectra on linear scales with (solid line) and without (dashed line) spectral broadening under a pump power of 300 mW. The inset shows the power spectra on semi-logarithmic scale. (b), (c): Pulse trains out of the grating in the cavity with and without spectral broadening.

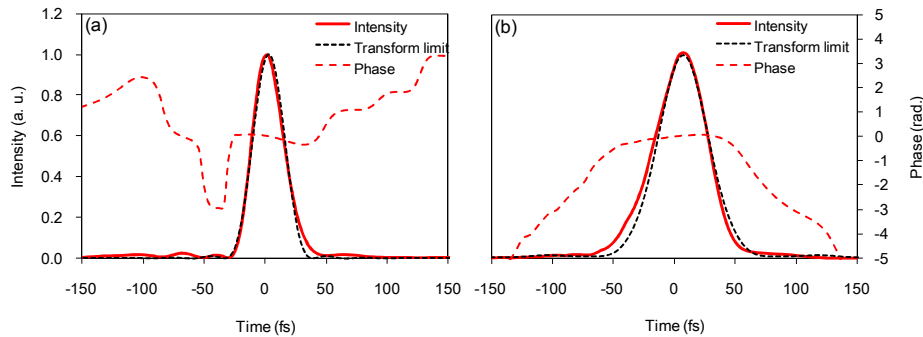


Fig. 3. Pulse intensity and phase profiles (solid and dashed lines, respectively) together with the transform-limited pulse shapes (dotted lines) for (a) the shortest pulse duration and (b) the pulse without spectral broadening.

3. Optimization of dispersion

It is important to understand the dispersion properties of the components in a laser oscillator. We measured the group delay dispersions ($GDDs = \partial^2 \phi(\omega) / \partial \omega^2$) of SMF, YDF and other optical components equivalent to those shown in Fig. 1. The transform-limited pulse shown in

Fig. 3(a) was propagated through these components one by one as a probe pulse. The change in spectral phase properties of the transmitted pulse was measured by SHG-CFROG to evaluate the GDD values in a wavelength range of 1000–1100 nm. The evaluated GDD of the SMF was $22.6 \text{ fs}^2/\text{mm}$ at 1060 nm. This value agreed reasonably well with the specification of the SMF. The GDD of the YDF provided by the manufacturer was $25.6\text{--}15.0 \text{ fs}^2/\text{mm}$ in the above wavelength region, whereas that experimentally measured was $37.3\text{--}29.8 \text{ fs}^2/\text{mm}$. This difference is most likely due to the 1030-nm absorption band of Yb. In addition to the signal absorption, the pump absorption might affect the dispersion properties of YDF. In our cavity setup, however, it is expected that the absorption-induced change of the GDD of YDF is not a significant effect due to the short fiber length. Figure 4(a) shows the evaluated GDDs of the 115-cm long SMF, 15-cm long YDF, GP1, GP2, and other components including a polarizing beam splitter and terbium gallium garnet crystal in the FI together with the net GDD of the cavity. As seen in this figure, the net GDD value is largely determined by the values of the SMF and GP1, and the slope of the net GDD may strongly depend on the SMF length. The slope of the wavelength-dependent net GDD in Fig. 4(a) is $-262 \text{ fs}^2/\text{nm}$.

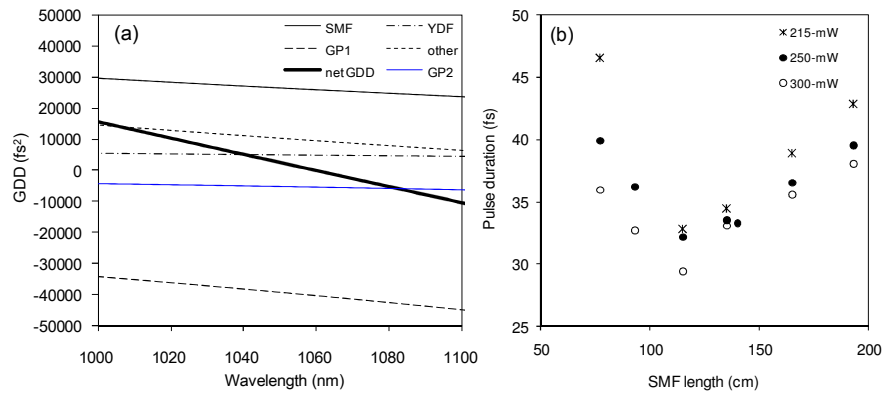


Fig. 4. (a) Measured GDD values of components in the cavity with a 115-cm long SMF. (b) Retrieved duration of compressed pulse as a function of the SMF length with a pump power parameter (215 mW (asterisk), 250 mW (closed circle), and 300 mW (open circle)).

We changed the total SMF length in a range of 77–193 cm by changing that of SMF1 in Fig. 1. Then the pulse repetition rate varied from 120 MHz to 77 MHz. Figure 4(b) plots the measured pulse durations as a function of the total SMF length with a pump power parameter set to 215, 250 and 300 mW. The GDD slope of GP2 was found to be $-20 \text{ fs}^2/\text{nm}$, which is smaller than that of the net GDD. The calculated slopes for SMF lengths of 77 cm and 193 cm were $-218 \text{ fs}^2/\text{nm}$ and $-352 \text{ fs}^2/\text{nm}$, respectively. One might expect a shorter pulse duration to be achieved by reducing the slope of the net GDD. Figure 4(b) suggests that the dependence of pump power on the pulse duration is relatively weak; however, there is an optimum fiber length for realizing a much shorter pulse. To understand this feature, we compared the details of the corresponding power spectra and the retrieved temporal profiles of intensity and phase for different SMF lengths in the case of 300-mW pumping, as shown in Fig. 5.

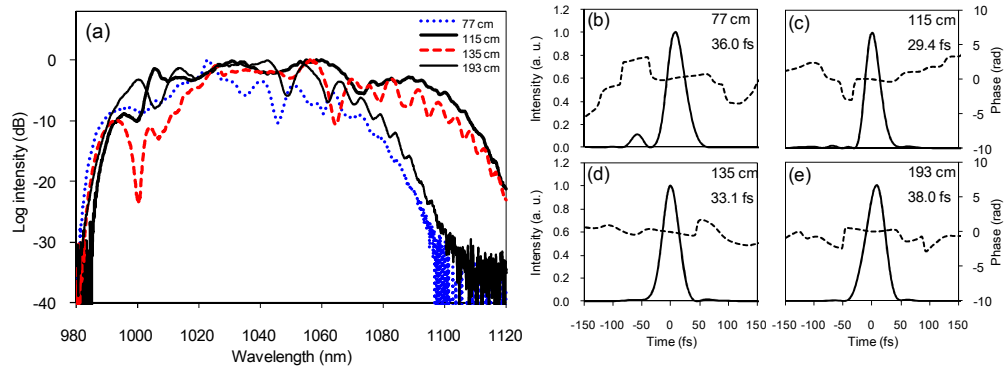


Fig. 5. (a) Power spectra. Pulse shapes and phases for SMF length of (b) 77 cm, (c) 115 cm, (d) 135 cm, and (e) 193 cm under a pump power of 300 mW.

Table 1. Dispersion Characteristics in the Cavity for Different SMF Lengths

SMF length [cm]	77	115	193
Net GDD @ 1050 nm [fs^2]	2.46×10^3	2.48×10^3	2.54×10^3
GDD slope [fs^2/nm]	-218	-262	-352
Max. nonlinear phase shift	0.86π	1.9π	3.0π

As the total SMF length was shortened from 193 cm, the spectral width increased as the phase variation was kept small (Figs. 5(c), 5(d) and 5(e)) to reach the maximum at 115 cm shown in Fig. 5(a). Then the shortest pulse duration of 29.4 fs was obtained. However, a very small pedestal structure caused by the residual TOD appeared before the main lobe as shown in Fig. 5(c). TOD, which affected the pulse shortening inside the cavity, was apparent in the case of 77 cm as seen in Fig. 5(b), suppressing the spectral broadening as indicated by a dotted line in Fig. 5(a). Furthermore, the SPM effect itself was reduced for shorter fiber lengths because the peak intensity of the intracavity pulses decreased with higher repetition rates. Therefore, a precise balance between reducing the GDD slope and increasing the SPM effect determines the optimal fiber length for the shortest pulse duration. Table 1 summarizes the dispersion characteristics in the cavity for different SMF lengths. The peak NPS values due to SPM estimated from the inferred temporal intensity profiles of the pulses in the cavity were 0.86π , 1.9π , and 3.0π for SMF lengths of 77, 115, and 193 cm, respectively. The static values of the net TODs in the cavity were evaluated to be 0.79×10^5 , 1.1×10^5 , and $1.6 \times 10^5 \text{ fs}^3$ at 1050 nm for SMF lengths of 77, 115, and 193 cm, respectively. Although the static TOD for the 193-cm long SMF was larger than that for the 77-cm long SMF, no significant pedestal structure can be observed for the former case. Because the NPS is proportional to the spectral intensity, the specific spectral shape can result in reversal of the sign of the TOD [16]. TOD due to the NPS caused by SPM was estimated by solving the nonlinear Schrödinger equation by the standard split-step technique using the measured spectrum and the estimated pulse profile at the inlet of SMF1. The estimated SPM-induced TODs were -0.06×10^5 , -0.28×10^5 , and $-0.65 \times 10^5 \text{ fs}^3$ at 1050 nm for SMF length of 77, 115, and 193 cm, respectively. These results indicate that the NPS contributes to the compensation of the residual TOD in the cavity and the resultant suppression of pedestal structures. Consequently, an optimal fiber length exists so that the NPS due to SPM compensates for the residual TOD in the cavity, resulting in a good temporal profile. However, the estimated TOD does not fully compensate for the net TOD, because other nonlinear effects such as nonlinear polarization evolution can lead to modulation of the temporal pulse profile and spectrum, which could also contribute a NPS.

4. Conclusion

In summary, we have optimized a mode-locked ytterbium-doped fiber oscillator. The shortest and cleanest pulse was easily produced without the use of additional optics for TOD compensation. We also investigated the dispersion properties in the oscillator by experimentally measuring GDDs of all of the components in the cavity. Reducing GVD by shortening the length of the fiber led to spectral broadening, resulting in the shortest pulse duration with an optimal fiber length. Such an optimum condition is determined by the SPM-induced compensation of the TOD of the cavity components and by a balance between the SPM-induced spectral broadening and the pulse broadening due to GVD. A simple layout for a mode-locked femtosecond oscillator with a clean temporal profile will be highly beneficial for many applications. We should also note that the stability of the pulses obtained from the oscillator was excellent (0.1% rms for more than one hour) because of the removal of complicated components, which is very important for industrial applications.